IOP Conf. Series: Materials Science and Engineering **307** (2018) 012083 doi:10.1088/1757-899X/307/1/012083

# Impact of the air gap at the casting/water-cooled-mold interface on casting microstructure

**Y D Zeng ,X F Li, Y Liu**

College of Materials Science and Engineering, Inner Mongolia University of Technology, Huhehaote,010051, China
E-mail: zyidan@sina.com

**Abstract.** In this paper, we report the results of experiments on gravity castings based on the experimental model of the controllable air gap. On basis of the temperature profiles at different locations of casting and mold were first measured, Beck's non-linear estimation procedure was applied to obtain the interfacial heat-transfer coefficient (IHTC) at the casting/mold interface. Using this as the boundary condition, the microstructures of the casting were simulated under different air-gap widths and formation time, which were compared to the microstructures of the measured casting. Furthermore, the impacts of the width of the air gap and the formation time of the air gap on the microstructure were analyzed. The results indicate that the air gap at the interface reduces the IHTC at the casting/mold interface, alters the solidification process of the casting, and has a great influence on the casting microstructure. Further, when the width of the air gap increases, the zone of the columnar grain of the casting decreases, the zone of the equiaxial grain is enlarged, and the columnar grains and equiaxial grains become coarser. When the formation time of the air gap increases, the zone of columnar grains of the casting is enlarged, the zone of the equiaxial grain is reduced, and the columnar grains and the equiaxial grains become finer.

## 1. Introduction

It is widely considered that a mold cooled by the circulating water (water-cooled mold) can rapidly exchange heat with a casting during the solidification process of the casting, which has a strong cooling effect on the casting. Thus, the microstructure of the obtained casting is fine, the segregation is slight, and the overall obtained mechanical performance is high. However, during the solidification process, an air gap will form at the casting/mold interface, which strongly hinders the heat exchange between the casting and the mold, thus greatly lowering the cooling effect of the mold and further affecting the solidification process and casting microstructure.

Casting microstructure has been a hot topic in related research, and as computer technology and mathematics have developed, the coupled cellular automata and finite-element method has become one of the major approaches in the investigation of microstructures. In recent years, a significant amount of related research has been reported[1–3].

Currently, for simulation of a microstructure, more studies focus on nucleation[4], dendritic growth [5], grain morphology[6], grain dimension[7,8] and the evolutionary process of microstructure morphology[2,9~10]. The influence of the formation of the air gap at the interface on the microstructure has been ignored. The impact of the air gap at the interface on the microstructure simulation of a sand mold casting may be neglected, but for metal casting and water-cooled casting the thermal resistance at the casting/mold interface caused by the interfacial air gap is far greater than the thermal resistance of the mold itself. Therefore, if the thermal resistance at the interface is neglected, a large deviation can occur in microstructure simulation results.

Therefore, in this paper we report the results of casting experiments based on the experimental model of the controllable air gap, of adopting the non-linear estimation method to obtain the interfacial heat-transfer coefficient (IHTC), and of determining the impact of the air gap on the IHTC. Based on such work, we performed simulations of a solidification microstructure and experimental studies that will help improve the accuracy of microstructure simulation.

## 2. Experiment

### *2.1 Experimental solution*

To study the impact of the air gap on the microstructure of a casting, the width of the air gap and the formation time of the air gap were chosen as the control factors in the experiments. The widths of the air gap were set as 0, 0.5, 1, and 2mm and the formation times of the air gap were set as 90 and 140s. Based on measured temperature, the non-linear estimation method was applied to obtain the IHTC. The IHTC was further used as the boundary condition for performing simulations of the solidification microstructure.

### *2.2 Experimental model*

As shown in Figure 1, the experimental model is a combined mold, in which one side is a movable water-cooled mold. The remaining portion is thermal insulation material. When molten metal is poured into the mold, the water-cooled mold moves towards the casting to closely contact the casting, such that no air gap is formed. When the solidification thickness reaches a preset value, the water-cooled mold is moved in the opposite direction, such that an air gap is manually formed at the interface. As a consequence, this model can accurately control the size and formation time of the air gap. A pressure sensor is installed on the push rod of the water-cooled mold, which can be relied on to accurately acquire the contact status between the water-cooled mold and the casting.

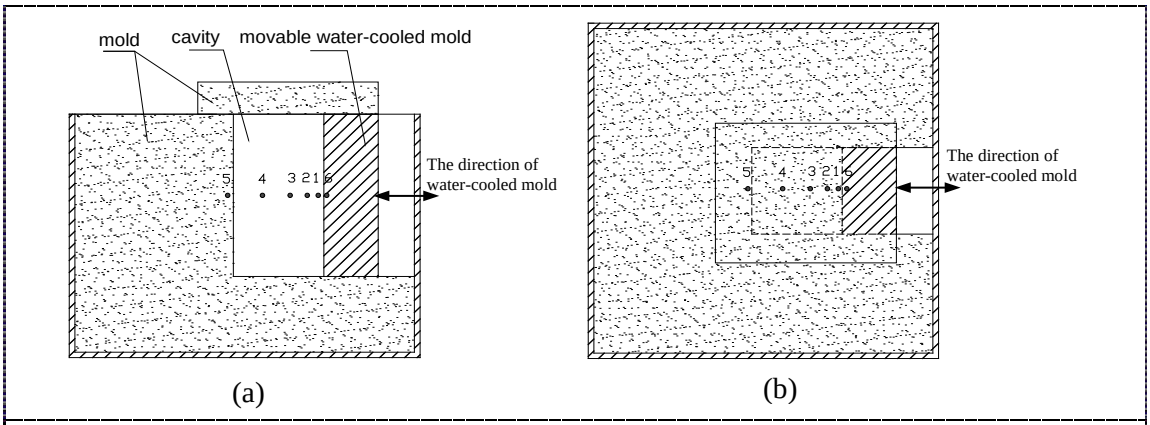


**Figure 1.** Experimental apparatus: (a) Front sectional view. (b) Horizontal sectional view.

### *2.3 Temperature measurement*

The distribution of temperature measurement points using thermocouples is shown in Figure 1, where points 1–4 represent points that are 5, 10, 30, and 50 mm, respectively, from the casting/water-cooled mold interface. Points 5 and point 6 are located in the mold and in the water-cooled mold, respectively, for measuring the temperatures of the walls of the mold and the water-cooled mold, respectively. K-type thermocouples with a wire diameter of 0.1mm are used for temperature measurements. In addition, the temperature at each measurement point is measured using an exposed thermocouple. The DAQ-USB-2401 module is utilized to collect data, the sampling frequency is 10Hz, and the temperature variation at each temperature measurement point is recorded during the experimental procedure.

### *2.4 Preparation of specimens*

The casting material is the industrial pure aluminum, the pouring temperature is controlled within 780–790°C, and the top gating system is applied. To observe the impact of the air gap on the microstructure of the casting, specimens are obtained at locations of the casting as illustrated in Figure 2 for preparation of the metallographic specimens.

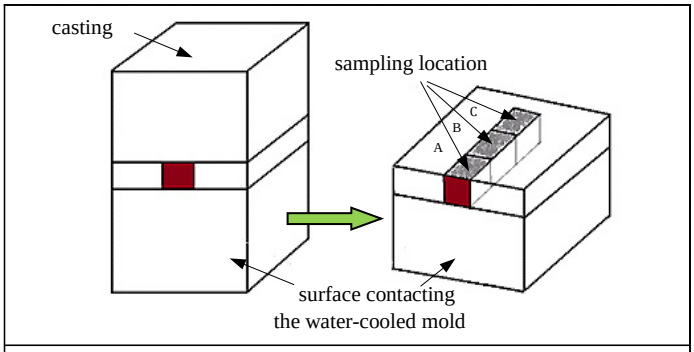


**Figure 2.** Sampling locations of metallographic specimens

## 3. Experimental results and analysis

### *3.1 Curves of measured temperature*

Figure 3 shows the temperature variation curves corresponding to the measurement points 1–6 under conditions of different air-gap formation times and different air gap widths. It can be seen that, without the air gap [Figure 3(a)], the curves of the temperature measurement points 1–4 inside the casting do not exhibit the phenomenon that the temperature decreases first and then increases, and the temperature reducing rate at each point is high. When the air-gap formation time is 90 s and the air gap width is 1 or 2 mm [see Figures 3(b) and 3(c)], the curves of the temperature measurement points 1–4 inside the casting first decrease rapidly and then increase, and the temperature reducing rate at each point is significantly lower than that without an air gap. Further, the wider the air-gap width, the higher the temperature recovery at the casting surface. This indicates that the heat exchange at the casting/water-cooled-mold interface occurs very quickly before the air gap is formed, and that the temperature at the surface of the casting decreases rapidly. After the air gap is formed, the air gap hinders the heat exchange between the casting/water-cooled mold, such that the heat exchange rate decreases, which results in the temperature recovery at the surface of the casting; that is, when the width of the air gap increases, the thermal resistance at the casting/mold interface increases. When the air-gap width is 2 mm, if the air-gap formation time increases from 90 to 140s, the temperature variance at each measurement point can be seen as shown in Figures 3(c) and 3(d). The temperature curves all show that the temperature first decreases, later increases, and then decreases again. As the air-gap formation time becomes longer, the amplitude of the temperature recovery is reduced. This is because the elongated air-gap formation time often indicates an elongated contact time between the casting and the mold, and the heat exchange between the casting and the mold decreases as the time increases, such that the impact of the air-gap formation on the cooling rate of the casting is reduced. Thus, the temperature recovery amplitude of the casting is relatively small.

### *3.2 Solution of the IHTC*

The non-linear estimation method proposed by Beck[11] is used to calculate the IHTC, and the result is shown in Figure 4. As the solidification time increases, the IHTCs under different conditions all display a decreasing trend. When there is no air gap, the IHTC is as shown in Figure 4(a). When the air-gap width is 1 mm, the IHTC decreases relatively slowly [as shown in Figure 4(b)], and when the air-gap width is 2 mm, the IHTC decreases rapidly [as shown in Figure 4(c)]. By comparing the three IHTC variation curves [Figures 4(a)–4(c)], it can be seen that when the air-gap width increases, the IHTC decreases, and the greater the air-gap width, the faster the IHTC decreases. Moreover, as the air-gap formation time increases, the IHTC is reduced [see Figures 4(c) and 4(d)].

### *3.3 Microstructure simulation and experimental results*

The CAFÉ module of PROCAST software is applied to simulate the casting microstructure, which is compared to that obtained by experimental casting.

#### *3.3.1. Microstructure*

The formation times of the air gaps are 90 and 140 s and the air-gap widths are 0, 1, and 2 mm. The

simulated microstructure of the cross-section of the casting is displayed in Figure 5, and, from the surface that contacts the water-cooled mold, four regions are found sequentially, which are the surface

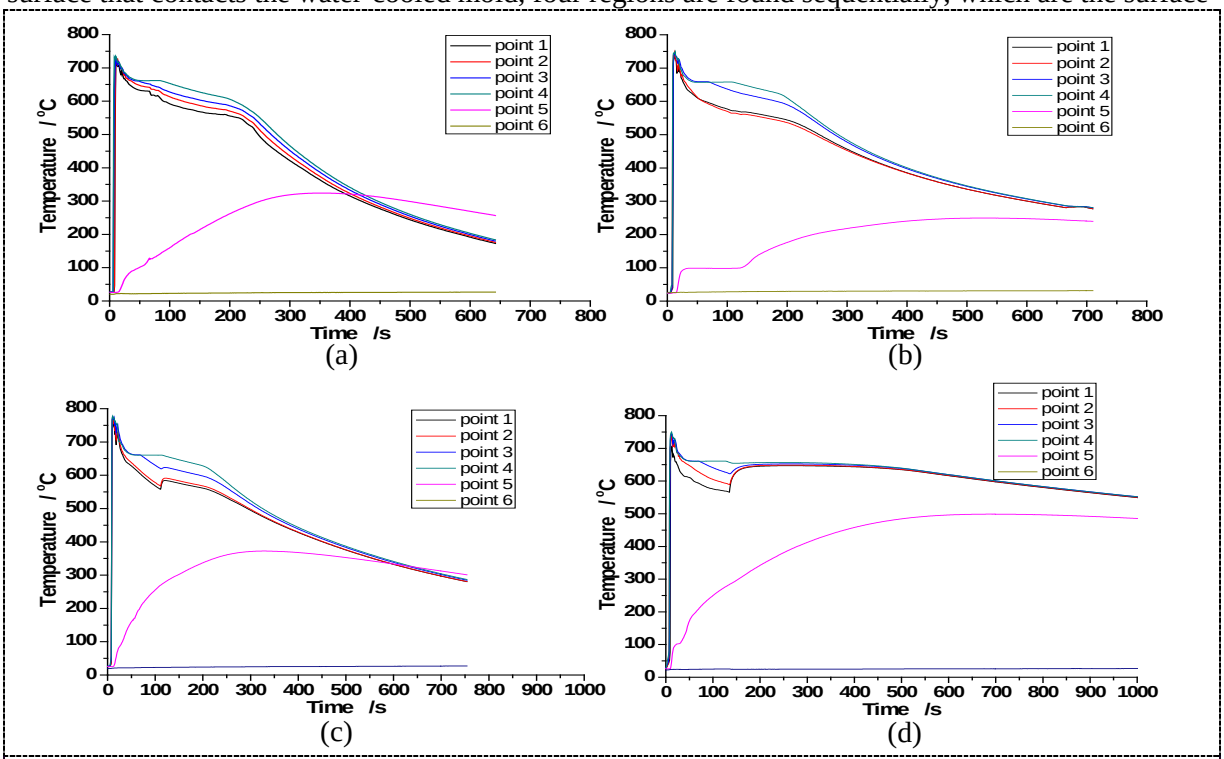


**Figure 3**. Measured temperature curves under different air gap widths and formation time

(a) no air gap (b) air-gap formation time 90 s and air-gap width 1 mm (c) air-gap formation time 90 s and air-gap width 2 mm (d) air-gap formation time 140 s and air-gap width 2mm

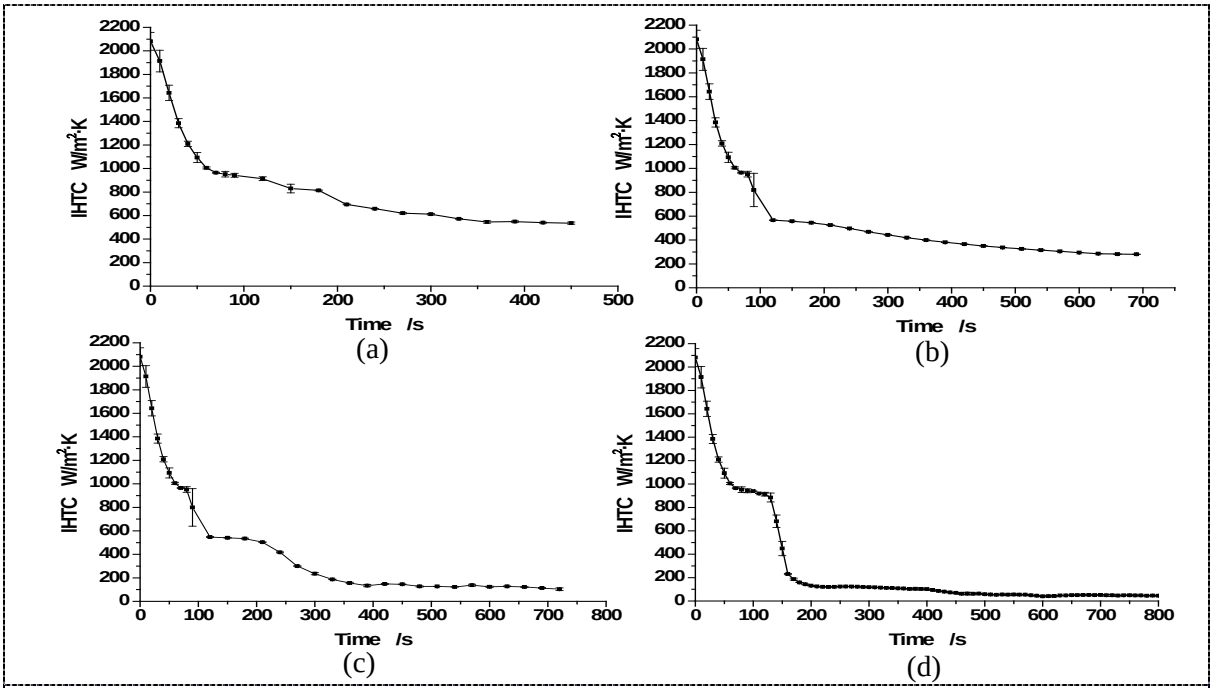


**Figure 4.** Calculation of IHTCs under different air-gap widths and formation time

(a) no air gap (b) air-gap formation time 90 s and air-gap width 1 mm (c) air-gap 90 s and air-gap width 2 mm (d) air-gap formation time 140 s and air-gap width 2mm

fine equiaxial grain zone, fine columnar grain zone, coarse columnar grain zone, and central coarse equiaxial grain zone.

Under the condition of the same air-gap formation time, as the air-gap width increases, the area of the columnar grain zone decreases and the columnar grains become coarser, the central equiaxial grain zone expands, and the grain size of the equiaxial grains increases significantly, as indicated in Figures 5(a)–(c). Under the condition of the same air-gap width, when the air-gap formation time increases, the area of the columnar grain increases and the columnar grains become finer, the equiaxial grain zone is reduced, and the grain size of the equiaxial grains decreases, as shown in Figures 5(c) and 5(d). The cooling effect of the water-cooled mold on the casting is far greater than the other five walls of the casting, and the heat dissipation of the casting mainly relies on the heat exchange between the casting and the water-cooled mold. Accordingly, the direction of heat exchange opposite the growth direction of the columnar grains is the main heat-flow direction.

Before the air gap is formed, the molten metal forms fine columnar grains under the strong cooling effect of the wall, and after the air gap is formed, as the air-gap width increases, the IHTC at the casting/mold interface decreases rapidly. Thus, the cooling effect of the mold on the casting decreases significantly, which weakens the heat exchange in the direction opposite the growth direction of the columnar grains. Consequently, the possibility that the grains grow in the form of equiaxial grains increases, which results in the contraction of the columnar grain zone and the expansion of the equiaxial grain zone.

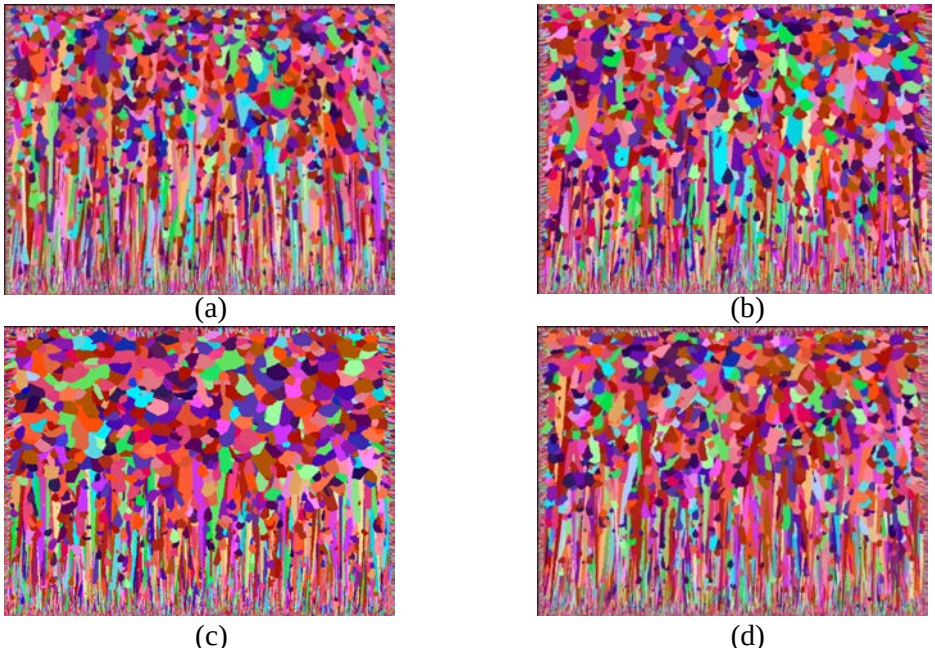


**Figure 5.** Simulated microstructures of casting cross-section

(a) no air gap (b) air-gap formation time 90 s and air-gap width 1 mm (c) air-gap formation time 90 s and air-gap width 2 mm (d) air-gap formation time 140 s and air-gap width 2mm

As the air-gap formation time increases, the contact time between the casting and the water-cooled mold increases. Specifically, the time that the casting/mold interface remains at a high IHTC is increased, and the heat exchange in a direction opposite the growth direction of the columnar grains weakens relatively slowly. Thus, the growth rate of the columnar grains is relatively fast, which results in an increase of the columnar grain zone and a reduction in the equiaxial grain zone.

*3.3.2. Cell spacing and grain size*

Given conditions where the air-gap formation time is 90 s and the air-gap widths are 0, 1, and 2 mm, the cell spacing is simulated and calculated results are obtained. When there is no air gap, the cell

spacing of fine columnar grains and coarse columnar grains are 32 and 112 um., respectively. After the air gap is formed, the cell spacing of coarse columnar grains increases significantly, the average value of which increases from 137 to 281 um, and the average grain size of the equiaxial grains increases from 261 to 499 um.. The air-gap formation causes the cooling rate of the casting to decrease significantly, and the cell spacing increases rapidly and correspondingly.

When the air-gap width is 2 mm, and the formation time of the air gap is 90 and 140s, the average distance between the coarse columnar grains is 281 and 123 um., respectively, and the average grain size of the equiaxial grains is 499 and 335 um, respectively. The longer the air-gap formation time, the longer the time the casting/mold interface remains at a high IHTC, such that the cooling rate of the casting is fast, which causes the columnar grains to be relatively fine.

In Figure 6, the air-gap width is 1mm and air-gap formation time is 90 s, the microstructures of the casting at the locations marked A, B, and C in Figure 2 are obtained, which indicates that the farther the microstructure is from the water-cooling interface, the coarser it is. Such a conclusion is consistent with the microstructure simulation. Under other conditions of the air-gap width, the microstructure of the casting shows similar behavior. The average cell spacing at locations A and B of the specimen are approximately 40 and 150um, respectively, and the average grain size at location C is 400um.

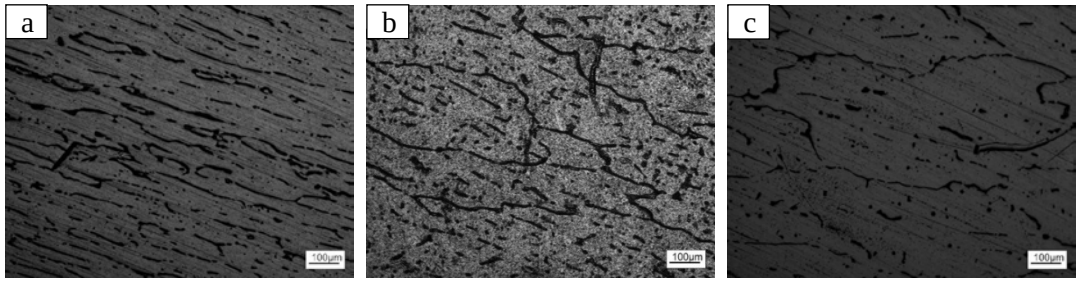


**Figure 6.** Measured microstructures of casting cross-section

(a) at locations A (b) at locations B (c) at locations C

## 4. Conclusions

The formation of the air gap at the casting/mold interface decreases the IHTC at the interface, resulting in a decreased cooling rate of the casting, which has a great impact on the casting microstructure. When the air-gap width increases, the IHTC decreases, and the change in the microstructure is that the area of the columnar grain zone decreases, the area of the equiaxial grain zone increases, and the columnar grains and equiaxial grains become coarser. When the air-gap formation time increases, the time that the casting/mold interface remains at the high IHTC becomes longer, the cooling rate of the casting becomes faster, the area of the columnar grain zone increases, the area of the equiaxial grain zone decreases, and the columnar and equiaxial grains become relatively finer.

## References

[1] Zaeem M A , Yin H B and Felicelli S D 2013 *Applied Mathematical Modelling* **37** 3495-503
[2] Vandyoussefi M and Greer A L 2002 *Acta Materialia* **50** 1693-705
[3] Gandin C A. and Rappaz M 1997 *Acta mater* **45** 2187-95.
[4] Seo S M, Kim I S , Jo C Y and, Ogi K 2007 *Materials Science and Engineering A* **449–451** 713-6
[5] Eshraghi M, Felicelli S D and Jelinek B 2012 *Journal of Crystal Growth* **354** 129-34
[6] Yin H and Felicelli S D 2010 *Acta Materialia* **58** 1455-65
[7] Omar L B , Uriel M H , José R and Christophe P 2017 *Materials & Design* **113** 369-76
[8] Reyes L A, Páramo P and Zamarripa A S 2015 *Materials & Design* **83** 301-7
[9] Han R H , Dong W C and, Lu S P 2014 *Computational Materials Science* **95** 351-61
[10] Zhang J W, Ou F L, Seufze Wand Taminge K . 2016 *Additive Manufacturing* **11** 32-9
[11] Beck J V and Blackwell B F 1985 *Inverse heat conduction Ill-posed problems*, Wiley, New York.